Uptake of ^{111}In-labeled fully human monoclonal antibody TSP-A18 reflects transferrin receptor expression in normal organs and tissues of mice

AYA SUGYO[1], ATSUSHI B. TSUJI[1], HITOMI SUDO[1], FUMIKO NOMURA[2], HIROKAZU SATOH[2], MITSURU KOIZUMI[3], GENE KUROSAWA[4], YOSHIKAZU KUROSAWA[4] and TSUNEO SAGA[1,5]

[1]Department of Molecular Imaging and Theranostics, National Institute of Radiological Sciences, Inage-ku, Chiba 263-8555; [2]Research and Development Division, Perseus Proteomics Inc., Meguro-ku, Tokyo 153-0041; [3]Department of Nuclear Medicine, Cancer Institute Hospital, Koto-Ku, Tokyo 135-8550; [4]Innovation Center for Advanced Medicine, School of Medicine, Fujita Health University, Toyoake, Aichi 470-1192; [5]Department of Diagnostic Radiology, Kyoto University Hospital, Shogoin, Sakyo-ku, Kyoto 606-8507, Japan

Received August 10, 2016; Accepted December 22, 2016

DOI: 10.3892/or.2017.5412

Abstract. Transferrin receptor (TfR) is an attractive molecule for targeted therapy of cancer. Various TfR-targeted therapeutic agents such as anti-TfR antibodies conjugated with anticancer agents have been developed. An antibody that recognizes both human and murine TfR is needed to predict the toxicity of antibody-based agents before clinical trials, there is no such antibody to date. In this study, a new fully human monoclonal antibody TSP-A18 that recognizes both human and murine TfR was developed and the correlation analysis of the radiolabeled antibody uptake and TfR expression in two murine strains was conducted. TSP-A18 was selected using extracellular portions of human and murine TfR from a human antibody library. The cross-reactivity of TSP-A18 with human and murine cells was confirmed by flow cytometry. Cell binding and competitive inhibition assays with [^{111}In]TSP-A18 showed that TSP-A18 bound highly to TfR-expressing MIAPaCa-2 cells with high affinity. Biodistribution studies of [^{111}In]TSP-A18 and [^{67}Ga] citrate (a transferrin-mediated imaging probe) were conducted in C57BL/6J and BALB/c-nu/nu mice. [^{111}In]TSP-A18 was accumulated highly in the spleen and bone containing marrow component of both strains, whereas high [^{67}Ga]citrate uptake was only observed in bone containing marrow component and not in the spleen. Western blotting indicated the spleen showed the strongest TfR expression compared with other organs in both strains. There was significant correlation between [^{111}In]TSP-A18 uptake and TfR protein expression in both strains, whereas there was significant correlation of [^{67}Ga] citrate uptake with TfR expression only in C57BL/6J. These findings suggest that the difference in TfR expression between murine strains should be carefully considered when testing for the toxicity of anti-TfR antibody in mice and the uptake of anti-TfR antibody could reflect tissue TfR expression more accurately compared with that of transferrin-mediated imaging probe such as [^{67}Ga]citrate.

Correspondence to: Dr Atsushi B. Tsuji, Department of Molecular Imaging and Theranostics, National Institute of Radiological Sciences, 4-9-1 Anagawa, Inage-ku, Chiba 263-8555, Japan
E-mail: tsuji.atsushi@qst.go.jp

Key words: monoclonal antibody, transferrin receptor, imaging, mouse, radiolabeling

Introduction

Transferrin receptor (TfR) is a type II transmembrane glycoprotein found as a homodimer (180 kDa) on the surface of cells, involved in iron uptake through interaction with transferrin and in regulation of cell growth (1,2). TfR is expressed at low levels on most normal cells, whereas it is expressed at higher levels on cells with high proliferation rates such as cancer cells (3-8). TfR is therefore an attractive molecule for targeted therapy of cancer. Many laboratories have developed various TfR-targeted therapeutic agents such as transferrin- and anti-TfR antibodies conjugated with anti-cancer agents (7,9). An antibody having high specificity and affinity to its target antigen is one of the most suitable agents to prepare drug-conjugates. Antibody-drug conjugate is initially tested in mice xenografted with human cancers to verify the selective delivery of the conjugate to tumor site and to validate non-specific tissue distribution. However, if the antibody reacts only with human antigen, it is not possible to verify the uptake to normal organs and tissues reflecting physiological antigen expression. Whether antigen expressed in normal tissues may or may not be accessible to blood-borne antibody-drug conjugates is not fully predictable by *ex vivo* immunohistochemical analysis. To predict the distribution in humans, especially the uptake in normal organs and tissues which is closely related to the toxicity of the antibody-drug conjugate, the use of an antibody that cross-reacts with murine antigen is essential. As

far as we know, there are no publications to date regarding such anti-human TfR antibodies (7,9).

In this study, to provide the biodistribution data of anti-TfR antibody in mice for predicting the biodistribution in human, we isolated a new fully human monoclonal antibody that can recognize both human and murine TfR from a large-scale human antibody library. Designated as TSP-A18, the cross-reactivity was evaluated using human and murine cell lines. It was radiolabeled with In-111 and the *in vitro* binding characteristics using a highly TfR-expressing cell line MIAPaCa-2, as well as the biodistribution in two murine strains C57BL/6J and BALB/c-nu/nu, were evaluated. Furthermore, the correlation of the uptake of radiolabeled antibody with TfR expression in major organs and tissues was analyzed, which was compared with the tissue distribution of [^{67}Ga]citrate.

Materials and methods

Antibody. The AIMS5 phage antibody library was used as a source of human monoclonal antibodies (10,11). The antigen used in the screenings of the library was prepared as follows: cDNA encoding a myc-His tagged extracellular portion of human TfR was inserted into an expression vector pCMV-Script (Clontech, Mountain View, CA, USA). The resultant plasmid DNA was transfected into 293T cells (American Type Culture Collection, Manassas, VA, USA) with Lipofectamine (Invitrogen, Carlsbad, CA, USA), and the transformants were grown in D-MEM medium (Sigma, St. Louis, MO, USA) supplemented with 10% fetal bovine serum. The extracellular portion of human TfR protein was purified from the supernatant of cell culture using Ni-NTA chromatography. We also prepared the murine antigen (extracellular portion of murine TfR) following the same procedure. The phage library selection process was described previously (12). In this study, the phage library was incubated alternately with immobilized human or murine antigen. Phages from individual colonies obtained after four rounds of panning were tested for binding to the extracellular portions of human and murine TfR by ELISA [the procedure was described previously (13)]. The nucleotide sequence of the positive clone was determined and the clone was designated as TSP-A18. It was subsequently converted to human IgG1 and the antibody was produced using Expi293 transient expression system (Thermo Fisher Scientific, Waltham, MA, USA). The antibody was purified with protein-A sepharose (ProteNova, Kagawa, Japan). An isotype control HR1-007 (11) was constructed in the same way.

Flow cytometric analysis. A human pancreatic cancer cell line MIAPaCa-2 and a mouse fibroblast cell line NIH/3T3 were purchased from American Type Culture Collection. The mouse B lymphocyte cell line Sp2/O, the human chronic myelogenous leukemia cell line K562, the mouse erythroleukemia cell line B8/3, the cynomolgus kidney derived fibroblast-like cell MK.P3(F) and the cynomolgus fetal spleen-derived T-cell like lymphocyte cell line HSC-F were purchased from Japanese Collection of Research Bioresources Cell Bank (Osaka, Japan). An insect cell line Sf9 derived from *Spodoptera frugiperda* was obtained from Thermo Fisher Scientific. Cells in suspension culture were harvested by centrifugation at 1,000 μg for 5 min. Adherent cells were removed from the dishes with EDTA-PBS (Thermo Fisher Scientific), then washed with PBS (Thermo Fisher Scientific). Cell density was adjusted at a concentration of $1x10^6$ cells/ml. TSP-A18 was serially diluted at concentrations of 0.002, 0.02, 0.2 and 2 μg/ml. An equal volume of the serially diluted antibodies was added to the cell suspensions and incubated for 1 h at 4˚C, followed by two washes with FACS buffer (1% BSA, 0.1% sodium azide, 2 mM EDTA in Dulbecco's PBS). The washed cells were incubated with mouse anti-human IgG (H+L) antibody labeled with Alexa 488 (Life Technologies Japan, Tokyo, Japan) as a second antibody for 1 h at 4˚C. The reacted cells were washed twice with FACS buffer and then measured by FACSCalibur (Becton-Dickinson, San Jose, CA, USA).

Radiolabeling. The antibody was conjugated with *p*-SCN-Bn-DOTA (DOTA) (Macrocyclics, Dallas, TX, USA) according to the procedure as described previously (14) with slight modifications. Briefly, during gentle shaking, a five molar excess of chelate in 13.7 μl DMSO was added to the antibody (10 mg in 1 ml 0.05 M bicine-NaOH, 150 mM NaCl, pH 8.5), and incubated for 17 h at 25˚C. Non-conjugated chelate was removed by size exclusion chromatography using a PD10 column (GE Healthcare, Little Chalfont, UK) and 0.1 M acetate buffer (pH 6.0) as eluent. The conjugation ratio of chelate to TSP-A18 was estimated to be ~3.5 by MALDI-TOF mass spectrometry. For In-111 labeling, 50 μg of DOTA-conjugated antibodies were mixed with 740 kBq of [^{111}In]Cl3 (Nihon Medi-Physics, Tokyo, Japan) in 0.5 M acetate buffer (pH 6.0) and the mixture was incubated for 30 min at room temperature. Radiolabeled antibodies were separated from free In-111 by Sephadex G-50 column (700 μg for 2 min once or twice). The labeling yields of [^{111}In]TSP-A18 ranged from 62.9 to 83.0%. The radiochemical purity of [^{111}In]TSP-A18 exceeded 97.5%. The specific activities of [^{111}In]TSP-A18 were 9.3-12.3 kBq/μg.

Cell binding and competitive inhibition assays. MIAPaCa-2 cells were maintained in D-MEM medium (Sigma) supplemented with 10% fetal bovine serum (Sigma). Cell binding and competitive inhibition assays were conducted as previously described (9). Briefly, cells were detached 3-4 days after seeding and cell suspensions were prepared. For cell binding assays, MIAPaCa-2 cells ($5.0x10^6$, $2.6x10^6$, $1.3x10^6$, $6.3x10^5$, $3.1x10^5$, $1.6x10^5$, $7.8x10^4$ and $3.9x10^4$) in PBS with 1% BSA (Sigma) were incubated with [^{111}In]TSP-A18 on ice for 60 min. After washing, the amount of cell-bound radioactivity was measured using a gamma counter (ARC-370M; Aloka, Tokyo, Japan). Immunoreactivity of [^{111}In]TSP-A18 was estimated according to the method of Lindmo *et al* (15). For competitive inhibition assays, [^{111}In]TSP-A18 were incubated with MIAPaCa-2 cells ($2.0x10^6$) in the presence of varying concentrations of the unlabeled intact TSP-A18, DOTA-conjugated TSP-A18, or HR1-007 as an isotype control (0, 0.3, 0.6, 3.0, 6.1, 30.3 and 60.6 nmol/l) on ice for 60 min. After washing, the amount of cell-bound radioactivity was measured. The dissociation constant (K_d) was estimated by applying data to a one-site competitive binding model using GraphPad Prism software version 6.0 for Mac (GraphPad Software, La Jolla, CA, USA).

Biodistribution of [^{111}In]TSP-A18 and [^{67}Ga]citrate. The animal experimental protocol was approved by the Animal Care and Use Committee of the National Institute of Radiological Sciences, and all animal experiments were conducted in accordance with the institutional guidelines regarding animal care and handling. Male C57BL/6J (19.3-23.3 g body weight) and BALB/c-nu/nu (15.4-19.4 g body weight) mice (Japan SLC, Hamamatsu, Japan) were intravenously injected with 37 kBq of [^{111}In]TSP-A18. The total injected protein dose was adjusted to 5 μg per mouse by adding the intact antibody. C57BL/6J (19.4-22.4 g body weight) and BALB/c-nu/nu (18.5-22.4 g body weight) mice were intravenously injected with 370 kBq of [^{67}Ga]citrate (Nihon Medi-Physics). At 1, 2, 4 and 7 days after injection of [^{111}In]TSP-A18, and at 2 h, and 1, 2 and 3 days after injection of [^{67}Ga]citrate, mice (n=5 at each time-point) were euthanized by excess isoflurane inhalation, and blood was obtained from the heart. Organs and tissues of interest (blood, lung, liver, spleen, pancreas, intestine, kidney, muscle and bone including marrow component) were removed and weighed. The radioactivity was measured using a gamma counter. The data were expressed as the percentage of injected dose per gram of tissue (% ID/g) normalized to a 20-g body weight mouse.

[^{111}In]TSP-A18 uptake in bone and bone marrow. On day 1 after i.v. injection of 37 kBq of [^{111}In]TSP-A18 into C57BL/6J and BALB/c-nu/nu mice (n=5 at each time-point), femur was removed, and then bone and bone marrow were separated and weighed. The radioactivity were measured using a gamma counter (ARC-370M; Aloka). The data were expressed as the percentage of injected dose per gram of tissue (% ID/g) normalized to a 20-g body weight mouse.

Western blotting for TfR protein expression. Western blotting was conducted as previously described (16). Briefly, blood, lung, liver, spleen, pancreas, intestine, kidney, muscle and bone marrow were removed from C57BL/6J and BALB/c-nu/nu mice (n=2), and the lysates were prepared using cell lysate buffer (Cell Signaling Technology, Danvers, MA, USA). The lysates were resolved by sodium dodecyl sulfate polyacrylamide gel electrophoresis, transferred to a polyvinylidene fluoride membrane (Hybond-P, GE Healthcare) and incubated with a rabbit anti-murine TfR antibody (ab84036, Abcam, Cambridge, UK) for 60 min at room temperature. After washing, the membrane was reacted with a horseradish peroxidase-linked anti-rabbit antibody (GE Healthcare) and visualized using an ECL Plus kit (GE Healthcare). Images were captured using a LAS-3000 imaging system (Fuji Film, Tokyo, Japan) and analyzed by ImageJ (National Institutes of Health, Bethesda, MD, USA). Two or three independent experiments for each C57BL/6J mouse and three for each BALB/c-nu/nu mouse were conducted.

Statistical analysis. The data of [^{111}In]TSP-A18 and [^{67}Ga]citrate in C57BL/6J and BALB/c-nu/nu mice were analyzed by the Student's t-test. The correlation between TfR protein expression and the uptakes of [^{111}In]TSP-A18 and [^{67}Ga]citrate, and between TfR protein expression and the area under the curve (AUC) of the uptakes was examined by simple regression analysis. AUC was calculated from the biodistribution data using the trapezoidal rule. A value of $P<0.05$ was considered statistically significant.

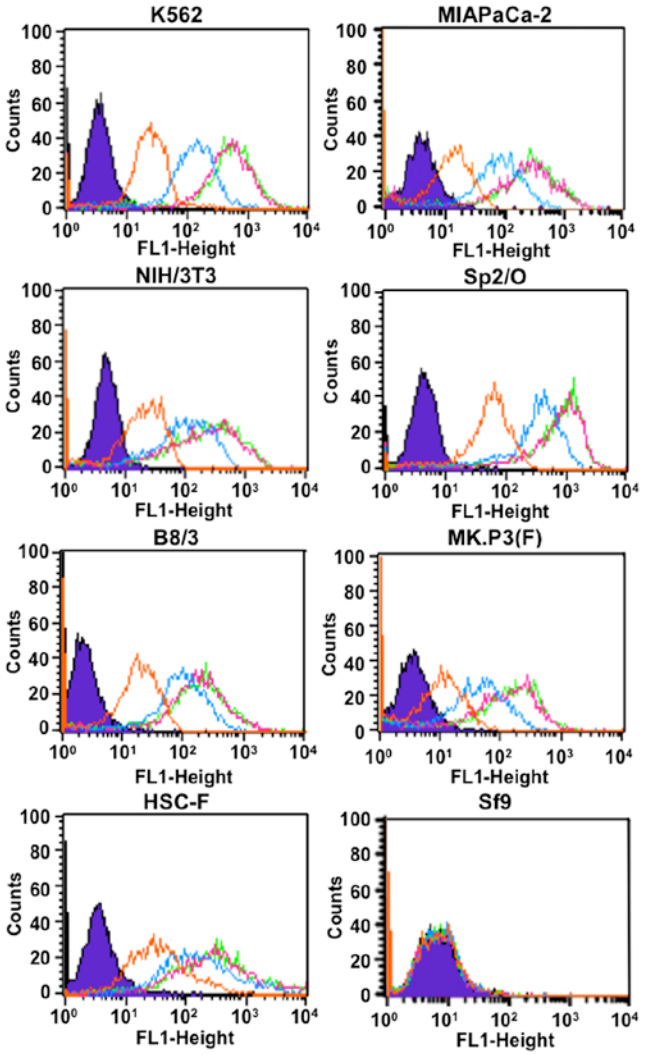

Figure 1. Flow cytometric analysis for cross-reactivity of TSP-A18 with human and murine TfR. TSP-A18 binding to human cells (K562 and MIAPaCa-2), murine cells (NIH/3T3, Sp2/O and B8/3), simian cells [MK.P3(F) and HSC-F] and insect cells (Sf9) was analyzed by FACSCalibur. Purple, 0 μg/ml of TSP-A18; orange, 0.001 μg/ml; blue, 0.01 μg/ml; pink, 0.1 μg/ml; green, 1 μg/ml.

Results

Flow cytometric analysis for cross-reactivity of TSP-A18. We selected a clone using extracellular portions of human and murine TfR from the AIMS5 phage library as a source of human antibodies (10,11). The clone was confirmed to bind to the extracellular portions of human and murine TfR as determined by ELISA (data not shown) and was designated as TSP-A18. The clone was converted to human IgG_1 and the antibody reacted with human cells (K562 and MIAPaCa-2) and murine cells (NIH/3T3, Sp2/O and B8/3), but not insect cells (Sf9) as determined by flow cytometry (Fig. 1). The intensity increased depending on TSP-A18 concentration and reached a maximum with TSP-A18 dose of 0.1 μg/ml or more (Fig. 1). The antibody TSP-A18 also reacted with simian cells [MK.P3(F) and HSC-F] as shown in Fig. 1.

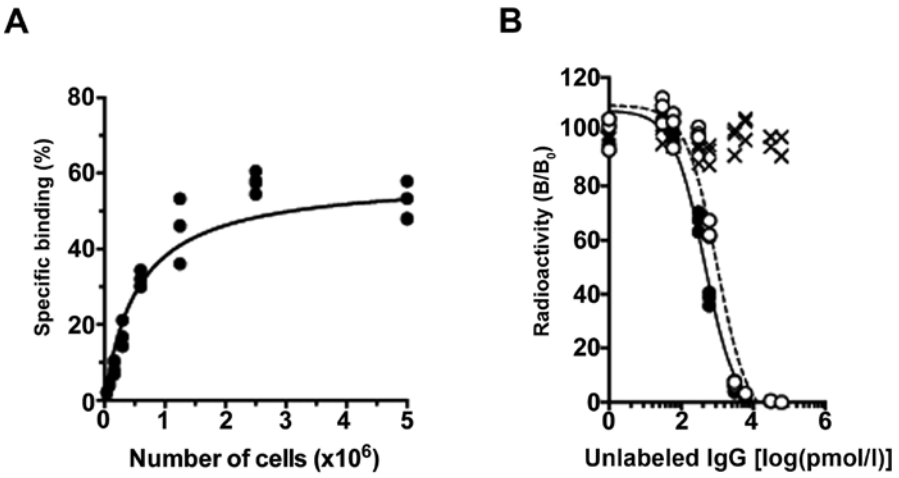

Figure 2. Cell binding and competitive inhibition assays for TSP-A18 using MIAPaCa-2 cells. (A) Cell binding assay of [^{111}In]TSP-A18 to MIAPaCa-2 cells. (B) Competitive inhibition assay for intact TSP-A18 (black circles, solid line), DOTA-conjugated TSP-A18 (white circles, dashed line) and HR1-007 (x, no line; isotype control) with MIAPaCa-2 cells.

Table I. Biodistribution of [^{111}In]TSP-A18 antibody in mice.

Strain	Day 1	Day 2	Day 4	Day 7
C57BL/6J				
Blood	5.4±0.7[a]	4.5±0.2[a]	2.2±0.3	0.7±0.1
Lung	2.7±0.2[b]	2.7±0.4[b]	2.6±0.1[b]	1.1±0.1[a]
Liver	3.6±1.4	2.9±0.8	4.7±0.6[b]	5.3±0.8[b]
Spleen	59.8±3.7[b]	64.3±5.0[b]	70.9±5.0[b]	65.7±7.9[b]
Pancreas	2.0±0.3[a]	2.0±0.4	2.1±0.3[b]	1.6±0.2[b]
Intestine	3.6±0.3[b]	2.2±0.4	1.9±0.2[b]	1.6±0.2[b]
Kidney	4.0±0.2[b]	3.2±0.2[a]	2.7±0.0[b]	2.2±0.1[b]
Muscle	1.2±0.4[a]	0.6±0.1	0.4±0.0[b]	0.3±0.1
Bone[c]	50.5±8.0[b]	34.5±4.1[b]	25.1±4.3[b]	16.2±2.7[b]
BALB/c-nu/nu				
Blood	4.4±0.5	3.8±0.6	2.0±0.1	0.6±0.0
Lung	2.0±0.2	1.8±0.26	2.1±0.2	1.0±0.1
Liver	2.5±0.7	3.0±1.6	3.0±0.4	3.4±0.5
Spleen	109.7±6.5	79.3±10.0	61.1±5.2	48.4±7.1
Pancreas	1.6±0.2	1.6±0.4	1.3±0.2	0.9±0.1
Intestine	1.9±0.3	1.9±0.5	1.5±0.1	0.9±0.2
Kidney	3.4±0.2	3.0±0.2	2.3±0.2	1.5±0.1
Muscle	0.7±0.1	0.7±0.2	0.5±0.0	0.3±0.0
Bone[c]	24.8±3.7	18.6±3.9	16.6±3.3	8.1±1.6

Data are expressed as % ID/g ± SD. [a]P<0.05, [b]P<0.01, when compared to BALB/c-nu/nu counterpart. [c]Bone containing marrow component.

Table II. Uptake of [^{111}In]TSP-A18 antibody on day 1.

Tissue	C57BL/6J	BALB/c-nu/nu
Bone containing marrow component	8.8±4.8	11.0±3.2
Bone marrow	188.0±27.5	104.8±24.5

Data are expressed as % ID/g ± SD.

Cell binding and competitive inhibition assays for TSP-A18. In the cell binding assay, [^{111}In]TSP-A18 bound highly to MIAPaCa-2 cells and the maximum value was >50% (Fig. 2A). From the competitive inhibition assay, K_d of intact TSP-A18 and DOTA-TSP-A18 were estimated to be 0.22 and 0.49 nM, respectively (Fig. 2B), suggesting that the loss of immunoreactivity by chelate conjugation was limited. In addition, HR1-007 as an isotype control did not inhibit TSP-A18 binding to TfR on the cell surface (Fig. 2B).

Biodistribution of [^{111}In]TSP-A18 in C57BL/6J and BALB/-nu/nu mice. Biodistribution experiments for [^{111}In] TSP-A18 were conducted in C57BL/6J and BALB/-nu/nu mice from days 1 to 7 after injection (Table I). Although [^{111}In] TSP-A18 highly accumulated in the spleen and bone containing marrow component of both C57BL/6J and BALB/-nu/nu mice, there were significant differences in the uptakes between the mice (Table I). [^{111}In]TSP-A18 uptake in the spleen of C57BL/6J and BALB/c-nu/nu mice at day 1 was 59.8±3.7% and 109.7±6.5% ID/g, respectively (Table I). The peak value of 70.9±5.0% ID/g in C57BL/6J mice was observed at day 4, whereas that of 109.7±6.5% ID/g in BALB/c-nu/nu mice was observed at day 1 (Table I). [^{111}In]TSP-A18 uptake in bone containing marrow component at day 1 was 50.5±8.0% ID/g for C57BL/6J mice and 24.8±3.7% ID/g for BALB/c-nu/nu mice (Table I). In another experiment, when [^{111}In]TSP-A18 uptake in bone and bone marrow was determined separately, most radioactivity was observed in the bone marrow of C57BL/6J and BALB/c-nu/nu mice (Table II).

TfR protein expression in organs and tissues. TfR protein expression in organs and tissues of C57BL/6J and BALB/c-nu/nu mice was determined using western blotting (Fig. 3).

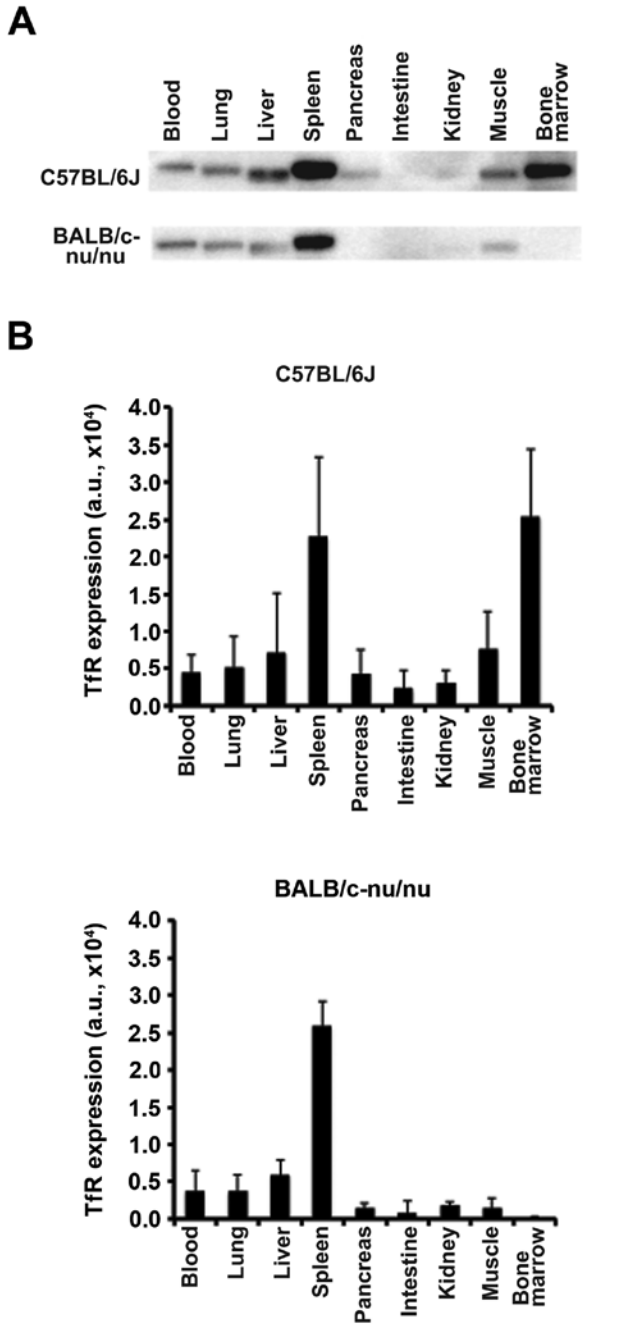

Figure 3. Western blot analysis of TfR protein expression. (A) TfR protein bands in tissues and organs (20 μg) of C57BL/6J and BALB/c-nu/nu mice are shown in upper and lower panels, respectively. (B) Densitometry of TfR protein bands. Data represent the mean and SD. au, arbitrary unit.

The spleen showed the highest expression compared with other organs in both C57BL/6J and BALB/c-nu/nu mice (Fig. 3). Although TfR protein was strongly expressed in the bone marrow of C57BL/6J mice, only a faint expression was observed in BALB/c-nu/nu (Fig. 3).

Biodistribution of [^{67}Ga]citrate in C57BL/6J and BALB/-nu/nu mice. Biodistribution experiments of [^{67}Ga]citrate were conducted in C57BL/6J and BALB/-nu/nu mice from 2 h to 3 days after injection (Table III). [^{67}Ga]citrate uptake in blood at 2 h was 17.0±1.3% ID/g for C57BL/6J mice and 15.4±0.9% ID/g for BALB/c-nu/nu mice and decreased with time (Table III).

Table III. Biodistribution of [^{67}Ga]citrate in mice.

Strain	2 h	Day 1	Day 2	Day 3
C57BL/6J				
Blood	17.0±1.3[a]	2.1±0.4[b]	0.7±0.1[b]	0.5±0.0[b]
Lung	6.8±0.6[a]	2.6±0.2[b]	1.9±0.1[b]	1.8±0.1[b]
Liver	4.0±0.4	6.0±1.4[a]	4.7±0.3	6.1±0.9[b]
Spleen	3.7±0.4	4.2±0.5[b]	4.4±0.2[b]	4.3±0.3[b]
Pancreas	4.7±0.5	4.9±1.0	4.9±0.3[b]	4.4±1.0[a]
Intestine	2.8±0.7[b]	2.3±0.4[b]	1.3±0.2[a]	1.0±0.1[b]
Kidney	6.5±0.7[b]	6.3±0.7[b]	5.6±0.4[b]	5.3±0.5[b]
Muscle	2.1±0.2	1.3±0.3[b]	1.0±0.1[b]	0.9±0.4
Bone[c]	12.2±1.1[b]	20.2±2.4	24.0±2.2[b]	20.5±2.0[a]
BALB/c-nu/nu				
Blood	15.4±0.9	1.0±0.4	0.4±0.1	0.2±0.1
Lung	6.0±0.6	1.6±0.4	1.4±0.1	1.3±0.1
Liver	4.4±0.4	4.8±0.5	5.1±0.7	4.8±0.5
Spleen	3.7±0.2	2.5±0.5	2.9±0.3	2.8±0.5
Pancreas	4.4±0.3	3.9±0.6	3.9±0.4	3.4±0.2
Intestine	1.7±0.3	1.0±0.3	0.9±0.2	0.5±0.1
Kidney	5.4±0.3	4.1±0.5	3.4±0.3	2.8±0.3
Muscle	2.0±0.2	1.2±1.1	0.6±0.1	0.6±0.1
Bone[c]	9.4±1.2	20.5±2.3	18.7±1.4	18.1±1.5

Data are expressed as % ID/g ± SD. [a]P<0.05, [b]P<0.01, when compared to BALB/c-nu/nu counterpart. [c]Bone containing marrow component.

[^{67}Ga]citrate uptake in containing marrow component at 2 h was 12.2±1.1% ID/g for C57BL/6J mice and 9.4±1.2% ID/g for BALB/c-nu/nu, and the peak values were 24.0±2.2% ID/g at day 2 for C57BL/6J and 20.5±2.3% ID/g at day 1 for BALB/c-nu/nu (Table III).

Correlation analysis. There were significant correlations between the TfR protein expressions and [^{111}In]TSP-A18 uptakes (all time-points and AUC) in both C57BL/6J and BALB/c-nu/nu mice (Fig. 4). There were significant correlations between the TfR protein expressions and [^{67}Ga]citrate uptakes (days 1, 2 and 3, and AUC) in C57BL/6J mice, whereas there was no correlation in BALB/c-nu/nu (Fig. 5).

Discussion

In this study, we isolated a new fully human antibody that recognizes the extracellular portions of human and murine TfR from a human antibody library and it was designated as TSP-A18. Flow cytometry confirmed that TSP-A18 recognizes TfR expressed on the surface of human and murine cell lines. Cell binding and competitive inhibition assays using [^{111}In]TSP-A18 showed high binding and affinity with TfR expressed on human cancer cells.

To our knowledge, there is no report to date on the distribution of anti-TfR antibody correlating with TfR expression on normal murine organs, although there are several reports

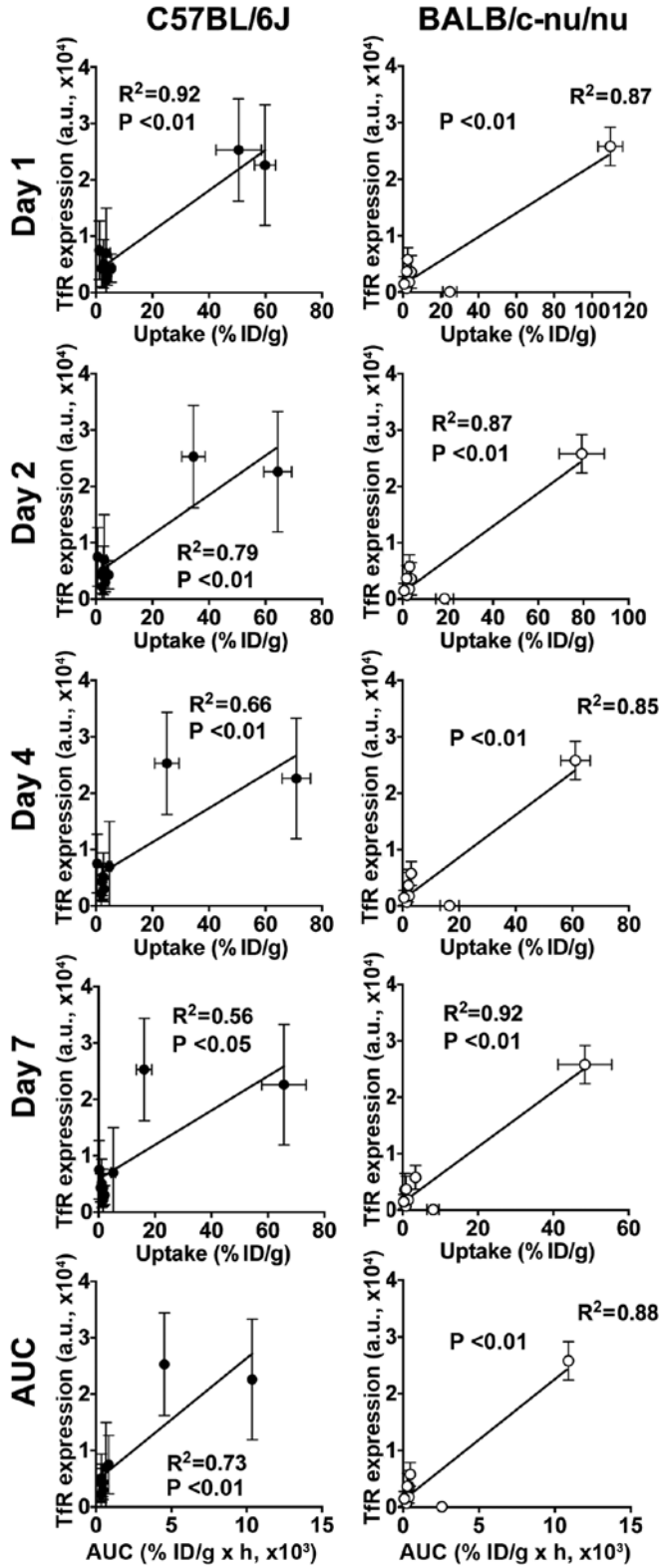

Figure 4. Correlation analysis of [^{111}In]TSP-A18 uptake and TfR protein expression in C57BL/6J (left panels) and BALB/c-nu/nu mice (right panels). The uptake and expression values were used in the biodistribution experiments (Table I) and western blot analysis (Fig. 3), respectively. au, arbitrary unit; AUC, area under the curve.

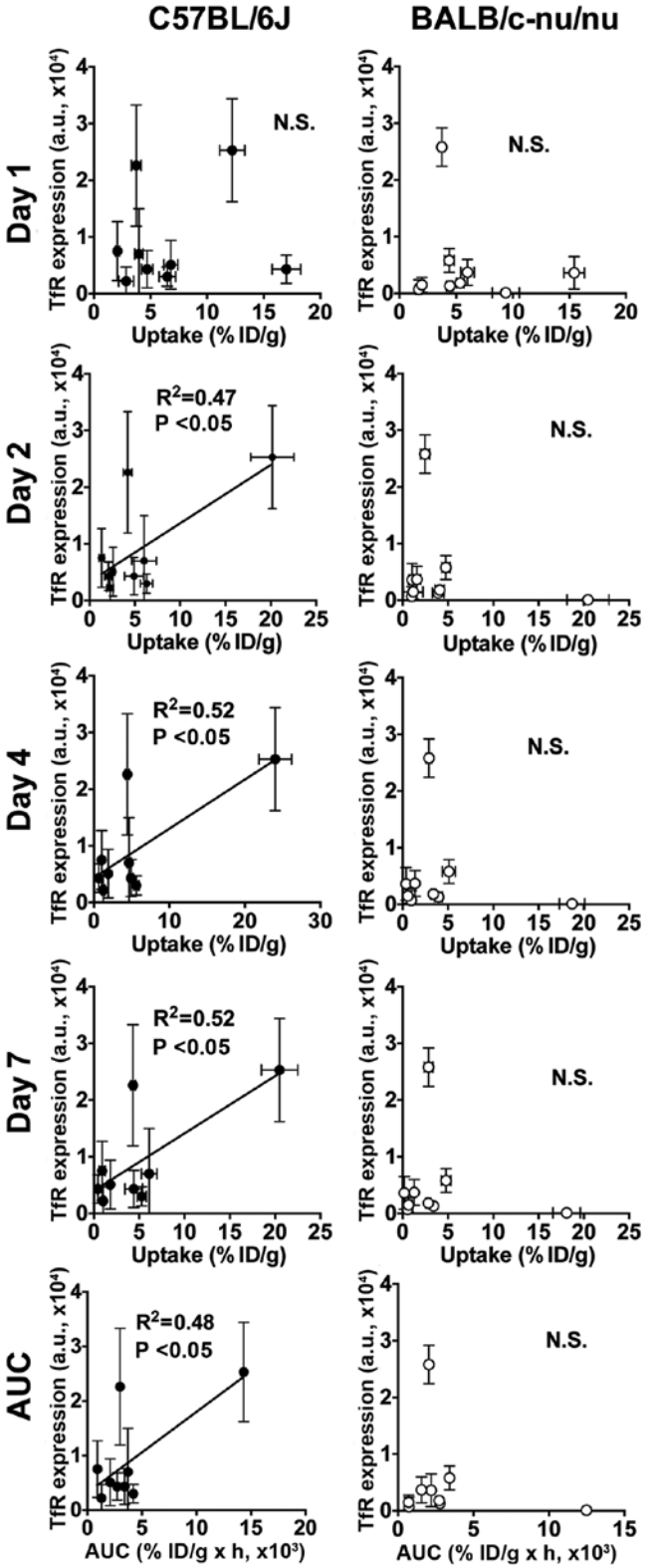

Figure 5. Correlation analysis of [^{67}Ga]citrate uptake and TfR protein expression in C57BL/6J (left panels) and BALB/c-nu/nu mice (right panels). The uptake and expression values were used in the biodistribution experiments (Table II) and western blot analysis (Fig. 3), respectively. au, arbitrary unit; AUC, area under the curve. NS, not significant.

on TfR-targeting via transferrin using [^{67}Ga]citrate or radiolabeled transferrin, in which biodistribution of these probes was evaluated in mice (BALB/c, BALB/c-nu/nu and FVB) and rats (Sprague-Dawley) (17-20). According to these reports, their uptakes in the liver and bone marrow were relatively high and those in the other organs and tissues including the spleen

were relatively low (17-20). Interestingly, our biodistribution experiments with [^{111}In]TSP-A18 in C57BL/6J and BALB/c-nu/nu mice showed that the highest uptake was observed in the spleen for both strains of mice, followed by that in bone containing marrow component. As mentioned above, splenic uptakes of [^{67}Ga]citrate and radiolabeled transferrin were not high (2.4-11.0% ID/g for mice and 0.3-1.2% ID/g for rats) (17,19,20). To confirm the reported biodistribution results on [^{67}Ga]citrate, biodistribution experiments of [^{67}Ga]citrate in C57BL/6J and BALB/c-nu/nu mice were conducted in this study. The biodistributions were similar to those in the previous studies (17-20), and the splenic uptakes were not high. In addition to the unexpectedly high uptake of [^{111}In]TSP-A18 in the spleen, there were marked differences in the uptake patterns in the spleen and bone containing marrow component between C57BL/6J and BALB/c-nu/nu mice. These findings raised the possibility that TfR expression levels in the murine tissues, especially the spleen and bone marrow are different between C57BL/6J and BALB/c-nu/nu mice. To test the possibility, TfR protein expression in major organs and tissues of C57BL/6J and BALB/c-nu/nu mice was determined by western blotting using a commercially available anti-TfR antibody and analyzed the correlation with the uptakes of [^{111}In]TSP-A18 and [^{67}Ga]citrate. The TfR protein expression levels in the spleen were markedly high for both strains, but the expression level in the bone marrow was high only for C57BL/6J mice. The differences in TfR expression may be a reason for the differences in the uptakes of [^{111}In]TSP-A18 in the two murine strains. There are significant correlations of TfR expression and uptakes of [^{111}In]TSP-A18 in both strains, whereas there are significant correlations of TfR expression with uptakes of [^{67}Ga]citrate only in C57BL/6J, but not in BALB/c-nu/nu. [^{67}Ga]citrate is also reported to accumulate in some transferrin-independent manner (21-23). These findings suggest that direct TfR-targeted imaging using radiolabeled anti-TfR antibody is more suitable for evaluating TfR expression in normal organs and tissues. TSP-A18 recognizes both human and murine TfR, therefore, radiolabeled TSP-A18 has the potential for imaging studies in human to assess the difference between directly TfR-targeted imaging and transferrin-mediated imaging such as [^{67}Ga]citrate.

In humans, [^{67}Ga]citrate accumulates mainly in the liver, moderately in bone marrow, and at lower levels in the spleen and other organs (24). However, this does not necessarily indicate low TfR expression in the human spleen, considering the results of this study as mentioned above. There are many reports of TfR protein expression in major human organs, tissues and tumors, and they showed high TfR expression in cells with high proliferation rate including some lymphocytes and monocytes in the bone marrow (5). However, to our knowledge, there are two studies on TfR expression in the spleen: one reported that frozen spleen sections were negatively stained as determined by immunohistochemical staining (4), and the other reported that only 2.5% of cells in the spleen were bound by anti-TfR antibody, whereas 40% of bone marrow cells were positive as determined by visual fluorescence assay (25). Taken together the TfR expression in humans described in the literature and the expression in mice that we determined in this study, there could be a marked difference in TfR expression in the spleen of humans and mice. This possible difference in TfR expression should be carefully considered when testing for the toxicity of anti-TfR antibody in mice.

TfR expression changes depending on the physiological status such as tumorigenesis (5). TfR is directly upregulated by MYC (26), which is an important mediator of cancer initiation and maintenance, and thought to be the cause of more than half of all human cancers (27,28). There is no MYC-targeted non-invasive imaging applicable to humans, whereas TfR is upregulated by MYC from the early stages of tumorigenesis (5,27,28). There is thus a potential role for TfR-targeted imaging to enable early detection of tumors. In addition, since increased expression of TfR correlates with tumor stage (7), TfR-targeted imaging could be a promising imaging method for staging. To demonstrate the concept, while it is not realistic to monitor TfR expression change with disease progression in each cancer patient, this should be feasible in carcinogenesis models such as genetically engineered and carcinogen-induced models (29). TfR is also reported to be upregulated by other factors such as phosphoinositide 3-kinase and hypoxia-inducible factor-1 (30,31). Temporal imaging for TfR expression change with disease progression in carcinogenesis models could be useful for clarifying role(s) of TfR in developing cancer and may provide clues for more efficient prevention, diagnosis and therapy of cancer. TSP-A18 labeled with gamma-ray or positron emitter could be used for monitoring in mouse models.

In conclusion, we developed a new fully human monoclonal antibody TSP-A18, which recognizes both human and murine TfR. [^{111}In]TSP-A18 accumulated highly in the spleen and bone marrow of C57BL/6J and BALB/c-nu/nu mice. This biodistribution pattern differed from that of [^{67}Ga]citrate, which accumulated highly in bone marrow, but not in the spleen. There was significant correlation between [^{111}In]TSP-A18 uptake and TfR protein expression in both strains, whereas there was significant correlation of [^{67}Ga]citrate uptake with TfR expression only in C57BL/6J. Radiolabeled TSP-A18 could be more suitable for evaluating TfR expression in normal organs and tissues of mice compared with [^{67}Ga]citrate.

Acknowledgements

This study was supported in part by KAKENHI 25861140. The authors appreciate the technical assistance of Yuriko Ogawa and Naoko Kuroda, and the staff in the Laboratory Animal Sciences section for animal management.

References

1. Neckers LM and Trepel JB: Transferrin receptor expression and the control of cell growth. Cancer Invest 4: 461-470, 1986.
2. Lesley JF and Schulte RJ: Inhibition of cell growth by monoclonal anti-transferrin receptor antibodies. Mol Cell Biol 5: 1814-1821, 1985.
3. Gatter KC, Brown G, Trowbridge IS, Woolston RE and Mason DY: Transferrin receptors in human tissues: Their distribution and possible clinical relevance. J Clin Pathol 36: 539-545, 1983.
4. Panaccio M, Zalcberg JR, Thompson CH, Leyden MJ, Sullivan JR, Lichtenstein M and McKenzie IF: Heterogeneity of the human transferrin receptor and use of anti-transferrin receptor antibodies to detect tumours in vivo. Immunol Cell Biol 65: 461-472, 1987.

5. Daniels TR, Delgado T, Rodríguez JA, Helguera G and Penichet ML: The transferrin receptor part I: Biology and targeting with cytotoxic antibodies for the treatment of cancer. Clin Immunol 121: 144-158, 2006.
6. Ryschich E, Huszty G, Knaebel HP, Hartel M, Büchler MW and Schmidt J: Transferrin receptor is a marker of malignant phenotype in human pancreatic cancer and in neuroendocrine carcinoma of the pancreas. Eur J Cancer 40: 1418-1422, 2004.
7. Daniels TR, Delgado T, Helguera G and Penichet ML: The transferrin receptor part II: Targeted delivery of therapeutic agents into cancer cells. Clin Immunol 121: 159-176, 2006.
8. Daniels TR, Bernabeu E, Rodríguez JA, Patel S, Kozman M, Chiappetta DA, Holler E, Ljubimova JY, Helguera G and Penichet ML: The transferrin receptor and the targeted delivery of therapeutic agents against cancer. Biochim Biophys Acta 1820: 291-317, 2012.
9. Sugyo A, Tsuji AB, Sudo H, Okada M, Koizumi M, Satoh H, Kurosawa G, Kurosawa Y and Saga T: Evaluation of efficacy of radioimmunotherapy with ^{90}Y-labeled fully human anti-transferrin receptor monoclonal antibody in pancreatic cancer mouse models. PLoS One 10: e0123761-e17, 2015.
10. Akahori Y, Kurosawa G, Sumitomo M, Morita M, Muramatsu C, Eguchi K, Tanaka M, Suzuki K, Sugiura M, Iba Y, *et al*: Isolation of antigen/antibody complexes through organic solvent (ICOS) method. Biochem Biophys Res Commun 378: 832-835, 2009.
11. Kurosawa G, Akahori Y, Morita M, Sumitomo M, Sato N, Muramatsu C, Eguchi K, Matsuda K, Takasaki A, Tanaka M, *et al*: Comprehensive screening for antigens overexpressed on carcinomas via isolation of human mAbs that may be therapeutic. Proc Natl Acad Sci USA 105: 7287-7292, 2008.
12. Morino K, Katsumi H, Akahori Y, Iba Y, Shinohara M, Ukai Y, Kohara Y and Kurosawa Y: Antibody fusions with fluorescent proteins: A versatile reagent for profiling protein expression. J Immunol Methods 257: 175-184, 2001.
13. Kurosawa G, Sumitomo M, Akahori Y, Matsuda K, Muramatsu C, Takasaki A, Iba Y, Eguchi K, Tanaka M, Suzuki K, *et al*: Methods for comprehensive identification of membrane proteins recognized by a large number of monoclonal antibodies. J Immunol Methods 351: 1-12, 2009.
14. Meares CF, Moi MK, Diril H, Kukis DL, McCall MJ, Deshpande SV, DeNardo SJ, Snook D and Epenetos AA: Macrocyclic chelates of radiometals for diagnosis and therapy. Br J Cancer (Suppl) 10: 21-26, 1990.
15. Lindmo T, Boven E, Cuttitta F, Fedorko J and Bunn PA Jr: Determination of the immunoreactive fraction of radiolabeled monoclonal antibodies by linear extrapolation to binding at infinite antigen excess. J Immunol Methods 72: 77-89, 1984.
16. Sugyo A, Tsuji AB, Sudo H, Nagatsu K, Koizumi M, Ukai Y, Kurosawa G, Zhang MR, Kurosawa Y and Saga T: Preclinical evaluation of ^{89}Zr-labeled human antitransferrin receptor monoclonal antibody as a PET probe using a pancreatic cancer mouse model. Nucl Med Commun 36: 286-294, 2015.
17. Chan SM, Hoffer PB, Maric N and Duray P: Inhibition of gallium-67 uptake in melanoma by an anti-human transferrin receptor monoclonal antibody. J Nucl Med 28: 1303-1307, 1987.
18. Vavere AL and Welch MJ: Preparation, biodistribution, and small animal PET of 45Ti-transferrin. J Nucl Med 46: 683-690, 2005.
19. Holland JP, Evans MJ, Rice SL, Wongvipat J, Sawyers CL and Lewis JS: Annotating MYC status with ^{89}Zr-transferrin imaging. Nat Med 18: 1586-1591, 2012.
20. Aloj L, Jogoda E, Lang L, Caracò C, Neumann RD, Sung C and Eckelman WC: Targeting of transferrin receptors in nude mice bearing A431 and LS174T xenografts with [^{18}F]holo-transferrin: Permeability and receptor dependence. J Nucl Med 40: 1547-1555, 1999.
21. Chen DC, Newman B, Turkall RM and Tsan MF: Transferrin receptors and gallium-67 uptake in vitro. Eur J Nucl Med 7: 536-540, 1982.
22. Chitambar CR and Zivkovic Z: Uptake of gallium-67 by human leukemic cells: Demonstration of transferrin receptor-dependent and transferrin-independent mechanisms. Cancer Res 47: 3929-3934, 1987.
23. Sohn MH, Jones BJ, Whiting JH Jr, Datz FL, Lynch RE and Morton KA: Distribution of gallium-67 in normal and hypotransferrinemic tumor-bearing mice. J Nucl Med 34: 2135-2143, 1993.
24. Jonkhoff AR, Plaizier MA, Ossenkoppele GJ, Teule GJ and Huijgens PC: High-dose gallium-67 therapy in patients with relapsed acute leukaemia: A feasibility study. Br J Cancer 72: 1541-1546, 1995.
25. Haynes BF, Hemler M, Cotner T, Mann DL, Eisenbarth GS, Strominger JL and Fauci AS: Characterization of a monoclonal antibody (5E9) that defines a human cell surface antigen of cell activation. J Immunol 127: 347-351, 1981.
26. O'Donnell KA, Yu D, Zeller KI, Kim J-W, Racke F, Thomas-Tikhonenko A and Dang CV: Activation of transferrin receptor 1 by c-Myc enhances cellular proliferation and tumorigenesis. Mol Cell Biol 26: 2373-2386, 2006.
27. Dang CV: MYC on the path to cancer. Cell 149: 22-35, 2012.
28. Li Y, Casey SC and Felsher DW: Inactivation of MYC reverses tumorigenesis. J Intern Med 276: 52-60, 2014.
29. Day C-P, Merlino G and Van Dyke T: Preclinical mouse cancer models: A maze of opportunities and challenges. Cell 163: 39-53, 2015.
30. Abe N, Inoue T, Galvez T, Klein L and Meyer T: Dissecting the role of PtdIns(4,5)P2 in endocytosis and recycling of the transferrin receptor. J Cell Sci 121: 1488-1494, 2008.
31. Tacchini L, Bianchi L, Bernelli-Zazzera A and Cairo G: Transferrin receptor induction by hypoxia. HIF-1-mediated transcriptional activation and cell-specific post-transcriptional regulation. J Biol Chem 274: 24142-24146, 1999.